Arabian Journal of Geosciences (2021) 14: 604
https://doi.org/10.1007/s12517-021-06888-9

ORIGINAL PAPER

Sedimentary geochemistry of the Weihe River sediments, Central China: implications for provenance and weathering

Xiaoxia Peng [1] · Congjun Feng [1] · Ling Guo [1,2]

Received: 3 January 2021 / Accepted: 3 March 2021 / Published online: 24 March 2021

Abstract

Modern river sediments sampled from the Weihe River, Central China, were analyzed in regard to facies, grain size, major and trace element, and rare earth element (REE). The main aim of the study was to investigate source rock provenance and paleoweathering intensity. Grain-size and outcrop analyses indicate that sediments from the Weihe River are predominantly slit (< 62 μm) and sand (62 μm to 2000 μm). Major and trace element concentrations show inverse correlations with SiO_2 content and grain size. Silty sediments are enriched in REE relative to upper continental crust (UCC), whereas sandy sediments tend to be depleted. UCC-normalized REE distribution fingerprints indicate that the silt sediments are mainly derived from the Loess Plateau, while sandy sediments are mainly sourced from the Qinling Mountains. Discrimination functions and La/Th ratio and Hf abundance discrimination diagram also show that silty sediments are mainly derived from quartzose sediments, the main components of Loess Plateau, while sandy sediments are mainly derived from felsic igneous source, the main components of Qinling Mountains in the region where tributaries flow. The chemical index of alteration (CIA), plagioclase index of alteration(PIA), and chemical index of weathering (CIW) suggest that Weihe River sediments are immature and have experienced relatively minor chemical weathering. This work has an important bearing on the general understanding of the role that source rock characteristics and weathering regime have on the formation of clastic sediments in modern rivers and provides a critical baseline for which future work on the Weihe River sediments can be evaluated against.

Keywords Modern river · Geochemistry · Paleoweathering · Provenance · China

Introduction

The chemical record of clastic sediments has been widely used for the determination of provenance and weathering in the source region (Bhatia 1983; Condie et al. 1992; Cullers 1988; Fedo et al. 1996; Feng and Kerrich 1990; McCann 1998; McLennan et al. 1983; Nesbitt et al. 1996; Tripathi et al. 2007). Particularly, the use of immobile major and trace elements, such as Al, Fe,Ti, Th, Sc, Co, and Zr, which are thought to be carried in the particulate load, and the rare earth elements (REEs), have been found to be useful indicators of the source (Taylor and McLennan 1985). The use of these immobile elements in provenance determination is based on the assumption that these immobile elements undergo little geochemical fractionation during denudational processes (Singh 2009). The immobile elements such as Al, Fe, Ti, Th, Sc, Co, and Zr and the REEs are commonly concentrated in the fine-grained sediments because their host minerals occur in that size range. Therefore, during the process of sediment transport and deposition, these immobile elements tend to concentrate in suspended load of the river leaving the bed-load sediments depleted in them. In contrast, coarse-grained sediments may show sorting effects, especially for zircon and Ti-oxidex (Manikyamba et al. 2008; Sugitani et al. 2006).

Responsible Editor: Attila Ciner

✉ Ling Guo
guoling@nwu.edu.cn

Xiaoxia Peng
pengxiaoxia2019@126.com

Congjun Feng
fengcj@nwu.edu.cn

[1] State Key Laboratory of Continental Dynamics, Department of Geology, Northwest University, 229 North Taibai Road, Xi'an 710069, Shaanxi, China

[2] Shandong Provincial Key Laboratory of Depositional Mineralization & Sedimentary Mineral, Shandong University of Science and Technology, Qingdao 266590, China

The weathering products of silicate rocks are particularly useful for evaluating continental weathering (Berner 1992; Gaillardet et al. 1999; Price and Velbel 2003; Velbel 1993). Rivers deliver an immense amount of weathered terrigenous matter to the sea, and this delivery plays a key role in earth surface process. The chemical weathering rates on continents are controlled by many factors, including the source rock type, climate regime, tectonic and topographic settings, vegetation, soil development, and human activities (Berner 1992; Gaillardet et al. 1999; Grantham and Velbel 1988; Meybeck 1987; Oliva et al. 2003; Stallard 1995). Various sediment geochemical proxies have been proposed to study the intensity of chemical weathering on continents primarily based upon the variable geochemical behavior of specific elements. Among these weathering indices, the chemical index of alteration (CIA; Nesbitt and Young 1982), the plagioclase index of alteration (PIA; Fedo et al. 1995), and the chemical index of weathering (CIW; Harnois 1988) are the most well-established methods for quantifying the degree of source weathering.

The Weihe River, which is the largest tributary of the Yellow River (China) located between Qinling Mountain and Loess Plateau, is an important source for potable water and agricultural irrigation in the Shaanxi province of northwest China. The region is well developed in industry and agriculture. Therefore, exploitation of building sands and the pollution of heavy metal and harmful element pollution in the Weihe River have attracted much attention (Lei et al. 2008; Li et al. 2014; Wang et al. 2011; Zhang et al. 2012b, c). In this study, we measured the contents of major elements, trace elements, rare earth elements (REEs), and grain-size distribution in the suspended and the bedload sediments of six outcrops, comprising 14 samples, from the lower Weihe River. Abundances of major and trace elements, along with REE concentrations, and viewed in light of sediment texture and grain size, are combined to evaluate the provenance and weathering intensity experienced by the source rocks of the Weihe River sediments. Therefore, the objectives of this study were to (1) investigate sedimentary characteristics of sediments in the Weihe River; (2) evaluate the sources of the sediments in Weihe River based on the correlations of major elements, trace element, and REE between possible source rocks and river sediments; and (3) evaluate the weathering intensity for the river sediments in Weihe River. This study has an important bearing on the general understanding of the role that source rock characteristics and weathering regime have on the formation of clastic sediments in modern rivers and provides a critical baseline for which future work on the Weihe River sediments can be evaluated against.

Geologic setting

The Weihe River, which is the largest tributary of the Yellow River (China), originates north of the Niaoshu Mountains of Weiyuan County, Gansu Province, and mainly flows through Tianshui of Gansu Province and Baoji, Xianyang, Xi'an, Weinan, and so on of Weihe Plain (also called Guanzhong Plain), Shaanxi Province (You et al. 2019). The Weihe Plain is important geographically and tectonically. It is adjacent to the Loess Plateau in the north and the North Qinling Mountains (NQM) in the south (Zhang et al. 2012a). It finally merges into the Yellow River at Gangkou Town, Tongguan County. The length of the river is 818 km, and the area drained covers 135,000 km^2 (Li et al. 2018). The Weihe River has several tributaries, including the Bangsha, Hei, and Feng rivers in the south and the Hulu, Jing, and Luo rivers in the north (Fig. 1). Passing through the Qinling Mountains and Loess Plateau, they carry sediment from multiple sources, including granitic rocks and older sedimentary rocks, as well as fine-grained sediments, from the Qinling Mountains and Loess Plateau, respectively. With the exception of limited water pollution and environmental assessment data on the Weihe River (Fan 2014), few geochemical studies focusing on the sediments have thus far been conducted, leading to a critical lack of context.

The Loess Plateau, to the north of the Weihe River, is dominantly composed of fine-grained silt, while to the south, the NQM are predominantly composed of igneous rocks, such as granite, as well as some older sedimentary units (Fig. 1; Guo et al. 2007; Liu et al. 2009; Zhang et al. 2001). Heavy loads of suspended sediments that are sourced from the Loess Plateau have led the Weihe River to have appeared yellowish in color. Tributaries to the north of Weihe River are generally longer, while southern branches originating from NQM are shorter but volumetrically provide a greater flux of water.

Sampling and analyses

Sampling was conducted during April of 2018, and a total of 14 field outcrop samples were collected using a plastic grab sampler. Sample location and lithologies are indicated in Fig. 1 and Table 1, respectively. Each sample collected was subsampled, and splits were subsequently used for grain size and geochemical analyses. Samples were stored in clean, sealed, polythene bags and then returned to the State Key Laboratory of Continental Dynamics, Northwest University.

A Malvern MS-2000 laser diffraction particle size analyzer was used to determine the grain-size distribution over the particle size range of 0.02 to 2000 μm. Particle size measurements were made by sieving the sediment to ensure a grain size of < 2000 μm. For geochemical analyses, sediment samples were powdered to 200 mesh in a tungsten carbide ball mill and then dissolved using an HF + HNO_3 mixture in Teflon bombs at 190 °C for 48 h. Trace elements and REE concentrations were measured on an Elan 6100 DRC inductively coupled plasmas mass spectrometer (ICP-MS) at the

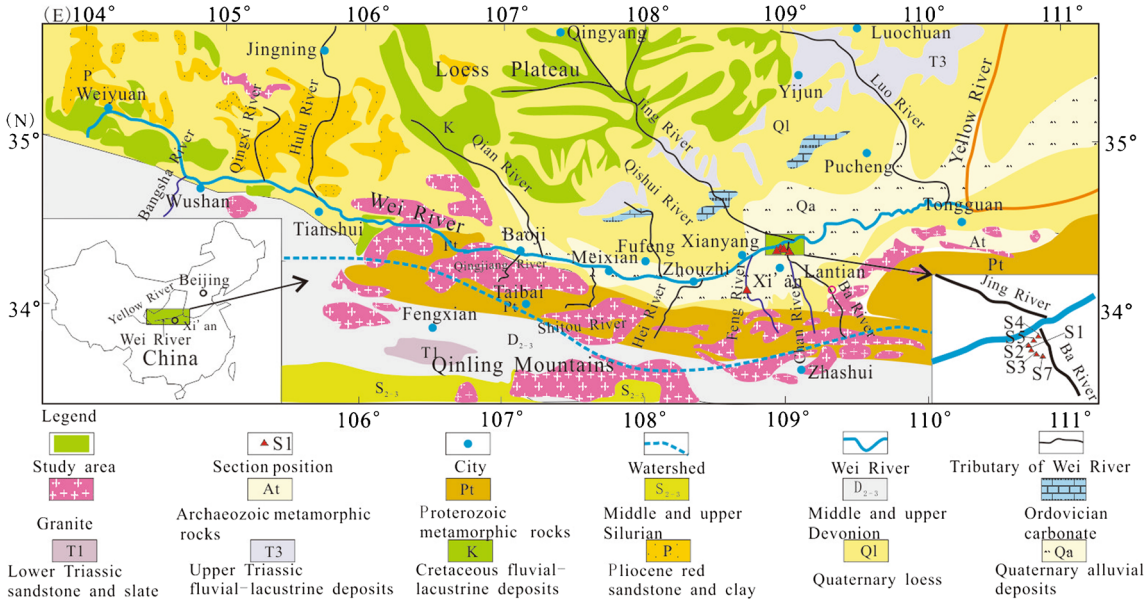

Fig. 1 Geologic map of the Weihe River catchment area showing distribution of the granitoids, loess, and sedimentary rocks. The tributaries of Weihe River and sample locations are also provided. The base map is modified after a geological map of the Qinling and Dabashan area (Zhang et al. 2001).

State Key Laboratory of Continental Dynamics, Northwest University, China, the detailed analytical procedure which is described by Liu et al. (2007). The analytical precision is estimated to be better than 5% for the majority of REE and trace elements, except for Be, Ga, Cs, Gd, and Th, which are estimated to be between 5 and 10%. Major elements were analyzed by X-ray fluorescence on a Rigaku RIX 2100 at the State Key Laboratory of Continental Dynamics, Northwest University, China, and analytical precision is better than 5%.

Facies and grain-size variations

Facies

Quaternary sediments deposited in the lower Weihe River consist of yellow and light grey sands, pebbly sands, silt, and muds (Fig. 2). Outcrops are exposed on the southern banks of the Weihe River, and sediments were sampled from outcrop sections at depths from 0.5 to 4.5 m (Fig. 2d). Sediments dominantly consist of stacked sets of moderately well-sorted fine-medium and coarse sands and are typically 0.3- to 1-m thick. Silt beds are commonly truncated by planar beds of sand and fine gravel (Fig. 2b). These sand bodies have local erosional bases and contain clearly defined graded bedding (Fig. 2b). Planar cross-bedded sets, with an average foreset dip of 30° and parallel bedding sets (Fig. 2a), are typically 0.3- to 0.8-m thick and can be traced laterally for tens of meters. Low angle to horizontally bedded fine sand and silts, approximately 0.6-m thick, were observed and typically overlie a coarse sand facies. Depositional structures include parallel bedding, cross bedding, and scour surface. Graded bedding in the pebbly and fine-medium sands within this unit indicates that they can be classed as a channel-fill facies (Galloway and Hobday 1996).

The remaining sediments within the Weihe River consist of light grey silt and muds. In exposed sections, the muddy-silt set is preserved in the middle of the vertical profile and displays horizontal bedding, indicating a weak hydrodynamic condition. Rain drop structures formed in the muds are also observed (Fig. 2c), indicating subaerial exposure. This unit is usually interbedded with cross and parallel bedded sandstones and is interpreted as an interchannel facies.

Grain-size variations

Grain-size parameters of fluvial sediments exposed in the different sedimentary facies that characterize this section of the Weihe River were analyzed to support the interpretation of geochemical variations. The coarse-grained (> 62 μm) sediments comprise the channel-fill facies, with fine sands (median size: 62 to 250 μm) mainly located at the top part of the section. The abundance of these fine sands varies within a range of 44–66.1% (Table 2). Sediments in the lower part of the section have a median size ranging from 250 to 2000 μm and are classified as medium to coarse sand. With regard to cumulative volume percentage, these medium to coarse sands vary from 42.2 to 44.9% for medium sands and 46% for coarse sands (Table 2). Fine-grained muds and silt, with a median size < 62 μm, account for 59.9–85.3% of the sediments (Table 2).

Table 1 Sampling details for the Weihe River sediments

Section no.	Sample ID	Lithology	Sample type	Sample location
Section 1	WXM1	Yellow fine and medium sands	Bed-load sediments, channel-fill deposits	N: 34° 25.8860′ E: 109° 00.1469′
Section 2	WXM2	Yellow fine and medium sands	Bed-load sediments, channel-fill deposits	N: 34° 25.8872′ E: 109° 00.1543′
Section 3	WXS3	Yellow medium and coarse sands	Bed-load sediments, channel-fill deposits	N: 34° 25.8504′ E: 109° 00.1630′
Section 4	WXM4-1	Yellow fine and medium sands	Bed-load sediments, channel-fill deposits	N: 34° 26.0117′
	WXM4-2	Light grey silt and fine sands	Suspended sediments, inter-fluve deposits	E: 109° 00.2353′
	WXM4-3	Yellow silt and fine sands	Suspended sediments, inter-fluve deposits	
	WXM4-4	Yellow medium and coarse sands	Bed-load sediments, channel-fill deposits	
	WXM4-5	Light grey silt and fine sands	Suspended sediments, inter-fluve deposits	
Section 5	WXM5	Yellow medium and coarse sands	Bed-load sediments, channel-fill deposits	N: 34° 25.9891′ E: 109° 00.1576′
Section 7	WXN7-2	Yellow medium and coarse sands	Bed-load sediments, channel-fill deposits	N: 36° 24.0742′
	WXN7-3	Yellow silt and fine sands	Bed-load sediments, channel -fill deposits	E: 109° 00.3186′
	WXN7-4	Yellow silt and fine sands	Suspended sediments, inter-fluve deposits	
	WXN7-5	Yellow medium and fine sandstone	Bed-load sediments, channel-fill deposits	
	WXN7-6	Light grey silt and fine sands	Suspended sediments, inter-fluve deposits	

Geochemistry

Major elements

The major element composition of the Weihe River sediments are provided in Table 3. In general, coarse-grained sands have moderate to high SiO_2 contents, with mean values between 71.88 and 74.57%, indicating a significant quartz component. Fine-grained sediments (mud to silt) tend to have lower SiO_2 contents, with a mean value of 67.52% (Table 3). The abundance of other major elements (Al_2O_3, Na_2O, K_2O, TiO_2, Fe_2O_3, MnO, MgO, CaO, and P_2O_5) are well correlated with SiO_2 (Fig. 3). In general, fine-grained samples have higher Al_2O_3, TiO_2, Fe_2O_3, MnO, MgO, CaO, and P_2O_5 compared to coarse-grained sediments. Negative linear relationships between SiO_2 and TiO_2, Fe_2O_3, MnO, P_2O_5, CaO, and MgO in the Weihe River sediments (Fig. 3) are likely attributable to most of the Si being sequestered in quartz, rather than as a clay component (Rahman and Suzuki 2007).

Following the physical and chemical weathering of source rocks, as well as transport prior to deposition, there is often a preferential enrichment of minerals, and their constituent elements, in the varying grain-size fractions (Sharma et al. 2013). Accordingly, the sediment geochemical composition tends to be a function of grain size (Whitmore et al. 2004). For example, SiO_2 in the medium to coarse sand samples has an average abundance of 74.7 ± 1%, whereas the fine to medium sands average of 71.9 ± 1.3%, and mud and silt samples average of 67.5 ± 2.1%. This indicates that SiO_2 content increases with larger grain sizes (Fig. 4). Similar trends are observed for several of the other major oxides, including Na_2O and K_2O. The average abundances of TiO_2, Fe_2O_3, MnO, MgO, CaO, and P_2O_5 tend to decrease with increasing grain size (Fig.4).

Trace elements

Trace element concentrations for Weihe River sediments are presented in Table 3. Trace element concentrations are normalized relative to upper continental crust (UCC) after Taylor and McLennan (1985). Relatively immobile trace elements, such as Cr and Ni, along with the major oxides Al_2O_3 and TiO_2, tend to undergo the least fractionation during sedimentary processes (Hessler and Lowe 2006). Several of the fine-grained samples (silt to fine sands mainly deposit in inter-fluve environment) are enriched in Li, Cr, Ni, Y, Zr, Cs, and Hf relative to UCC, while other trace elements such as Be, Sc, V, Cu, Zn, Ga, Ge, Rb, Sr, Nb, Th, and U are depleted relative to UCC (Fig. 5). Fine to medium sands samples (deposits mainly at the upper or edge of the channel) are enriched in Co, Ba and Pb relative to UCC, while other trace elements such as Li, Be,V, Sc, Cu, Zn, Ga, Ge, Sr, Y, Zr, Nb, Hf, Th, and U are depleted relative to UCC (Fig. 5). Medium to coarse sand samples (deposits mainly at the bottom of the channel) are enriched in Co, Ba, and Pb relative to UCC, while other trace elements such as Li, Be, Sc, V, Ni, Cu, Zn, Ga, Ge, Y, Nb, Cs, Hf, Ta, Th, and U are depleted relative to UCC (Fig. 5). All of the Weihe River samples are depleted in Cr and Ni relative to world sediment (WS) (Cr, 74 ppm; Ni, 40 ppm; McLennan 1995). The concentration of trace elements in river sediments are the result of the competing influences of source

Fig. 2 Characteristics of Quaternary sediments from the Weihe River and its tributaries. **a** Yellowish fine and medium sands with parallel and cross-bedding structures. These represent the channel-fill deposits in Section 2 of the Weihe River. **b** Yellow coarse and medium sands with a scour surface on top, and muddy silt on the bottom, interpreted as channel-fill and inter-fluve deposits, Section 4 (WXM4), Weihe River; **c** light grey weakly consolidated mudstone with rain drop structures and are inter-fluve deposits, on top of Section 10, Weihe River; **d** macroscopic outcrops picture of Section 7, Weihe River; **e** sandy conglomerate, the fine gravels are dominantly composed of granite, Feng River (location: N 34° 12′ 48.0″; E 108° 44′ 14.9″); **f** conglomerate, the gravel are mainly composed of granite, Ba River (location: N 34° 25′ 28.3″, E 109° 00′ 35.8″). Locations of sections are listed in Table 1.

rock properties, weathering, diagenesis, sediment sorting, and the aqueous geochemistry of individual elements (Rollinson 2014).

The effect of physical sorting of sediments often has the most significant impact on trace element concentrations (Singh 2009). Trace element concentrations in the Weihe River sediments are close to those of UCC except for Sc, V, Co, Cu, Zn, Nb, Ba, Hf, and U in the coarse-grained sediments and Co and Zr contents in the fine-grained sediments (Fig. 5). Furthermore, coarse-grained sediments typically have trace element concentrations lower than the fine-grained sediments (Table 3 and Fig. 5). The high trace element concentrations in fine-grained sediments suggest that elemental enrichments may be associated with the presence of clay minerals (Konhauser et al. 1998; Konhauser et al. 1994; Kronberg et al. 1979). The depletion of Sr and Nb is attributed to the dilution effect that SiO_2 has in mud and silt sediments (Bhuiyan et al. 2011; Tripathi et al. 2007).

Rare earth elements

Rare earth element (REE) concentrations and several characteristic ratios for Weihe River sediments are provided in Table 3, and concentrations for the paleosol and loess of the Loess Plateau and granite of the Hei River are listed in Table 4 for comparison. Fine-grained particles, such as clay minerals, are important vectors for REE (Taylor and McLennan 1985). The total REE (ΣREE) concentrations of Weihe River sediments show wide variations, ranging from 65.78 to 166.74 ppm, with an average 118.8 ppm. Most samples have ΣREE concentrations below that of UCC (146.37 ppm; Taylor and McLennan 1985), and only four samples display enrichments relative to UCC.

The LREE/HREE (light rare earth element/heavy rare earth element) ratio varies between 8.03 and 9.87, with a mean of 8.81. Normalized Eu anomalies (Eu/Eu*) were calculated as $Eu/Eu^* = Eu_N/(Sm_N + Gd_N) \times 1/2$ (Taylor and McLennan

Table 2 Particle size distribution, cumulative percent by volume, and median grain size of the Weihe River sediments

Sample ID	Cumulative volume percentage (%)						Median
	< 4 μm Muds	4–62 μm Silt	62–250 μm Fine sands	250–500 μm Medium sands	500–2000 μm Coarse sands	> 2000 μm Conglomerate*	(μm)
WXM1	0.5	9.3	53.3	31.7	5.2	Null	193.8
WXM2	0.8	8.2	44.1	39	7.9	Null	229.3
WXS3	0.7	3	7.8	40.6	46	Null	466.2
WXM4-1	0.5	3.6	61.1	22.2	12.6	Null	184.3
WXM4-2	4.5	78.6	16.5	0.4	–	Null	34.1
WXM4-3	5.2	80.1	14.7	0	–	Null	33.5
WXM4-4	1.5	14.3	16.3	44.9	23	Null	326
WXM4-5	1.9	52.3	38.3	2.4	5.1	Null	56.4
WXM5	–	2.4	22.1	43.1	32.4	Null	370
WXN7-2	–	4.5	16.2	42.9	36.4	Null	399.9
WXN7-3	–	34	33.5	20.1	1.4	Null	58.5
WXN7-4	1.8	51.1	44	2.7	0.4	Null	57.6
WXN7-5	–	8.6	28.8	42.2	20.4	Null	298.8
WXN7-6	3.7	63.3	29.3	2.9	0.8	Null	43.9

Conglomerate: Conglomerate contents cannot be detected in Malvern MS-2000 laser diffraction particle size analyzer

"-" presents an undetectable value

1985), with values ranging from 0.94 to 1.39, and a mean of 1.12. Cerium anomalies (Ce/Ce*) were calculated following the formula $Ce/Ce^* = Ce_N/(La_N + Pr_N) \times 1/2$ (Taylor and McLennan 1985) (subscript N denotes a normalized concentration, and for this paper, the normalizing values are chondrite; Haskin et al. 1966). Cerium anomalies vary from 0.85 to 0.97, with a mean of 0.91. Chondrite-normalized REE distribution patterns for the Weihe River sediments (Fig. 6a and b) (Haskin et al. 1966) display strong LREE enrichments relative to the HREE. The REE distribution patterns can be divided into two groups, fine-grained samples (WXM4-2, WXM4-3, WXM4-5, WXN7-3, WXN7-4, and WXN7-6) that display negative Eu anomalies and HREE enrichments about 10 times greater than chondrite values (Fig. 6a). Chondrite-normalized patterns of the fine-grained sediments are similar to averaged sediment sources known from the Loess Plateau, including a paleosol (S_{ave}, $n = 8$) and loess sample (L_{ave}, $n = 7$) (Ding et al. 2001). Coarse-grained samples (WXM-1, WXM-2, WXS3, WXM4-1, WXM4-4, WXM5, WXN7-2, and WXN7-5) display a slight positive Eu anomaly and a similar LREE enrichment as observed for the fine-grained sediments (Fig. 6b). Chondrite-normalized patterns of these coarse-grained sediments are similar to the average REE composition of the granite upstream of the Hei River (HG_{ave}, $n = 8$), a tributary of Weihe River (Fig. 1). Relative to chondrite values, La has a maximum enrichment between 51 and 117 times, while Ho ranges between 4 and 15 times, and La_N/Yb_N ratios range between 0.9 and 1.22, highlighting the strong LREE enrichment.

Rare earth element patterns were also normalized with respect to UCC after Taylor and McLennan (1985). Average UCC serves as an appropriate estimate for the average source rock composition (Mao et al. 2014) and is widely used to normalize REE concentrations in sedimentary samples (Mao et al. 2014; Singh 2009). Weihe River sediments can be divided into two groups based on their UCC-normalized REE patterns (Fig. 6c and d). The fine-grained samples (WXM4-2, WXM4-3, WXM4-5, WXN7-3, WXN7-4, and WXN7-6) are characterized by REE abundances close to those of UCC (Fig. 6c) and are similar to UCC-normalized values for S_{ave} and L_{ave} (Ding et al. 2001). In contrast, coarse-grained samples (WXM-1, WXM-2, WXS3, WXM4-1, WXM4-4, WXM5, WXN7-2, and WXN7-5) are depleted relative to UCC, and similar to HG_{ave}.

Discussion

Provenance

REE distribution fingerprints are an important tracer for source rocks, as REE are relatively immobile during weathering and diagenetic processes (McLennan 1993). The distribution patterns of the Weihe River sediments can be

Table 3 Major, trace, and rare earth element compositions of the Weihe River sediments

	WXM1	WXM2	WXS3	WXM4-1	WXM4-2	WXM4-3	WXM4-4	WXM4-5	WXM5	WXN7-2	WXN7-3	WXN7-4	WXN7-5	WXN7-6	UCC	WS
	Sfm	Sfm	Smc	Sfm	Fms	Fms	Smc	Fms	Smc	Smc	Fms	Fms	Smc	Fms		
Major oxide (wt%)																
SiO_2	71.16	73.35	76.12	71.14	65.26	65.98	73.14	68.56	75.37	74.18	70.93	68.19	74.04	66.17	65.89	64.2
TiO_2	0.27	0.32	0.18	0.32	0.62	0.62	0.31	0.57	0.22	0.18	0.48	0.55	0.36	0.62	0.5	0.75
Al_2O_3	10.74	10.07	10.79	10.28	11.11	10.74	10.41	9.68	10.48	10.79	9.46	9.73	9.75	10.71	15.17	13.42
TFe_2O_3	1.99	1.97	1.44	2.24	3.6	3.45	2.02	2.96	1.51	1.42	2.53	2.88	2.39	3.44	4.49	5.72
MnO	0.05	0.04	0.03	0.05	0.07	0.07	0.04	0.06	0.03	0.03	0.06	0.06	0.04	0.07	0.07	0.09
MgO	0.96	0.83	0.61	1.01	1.93	1.88	0.87	1.37	0.64	0.63	1.15	1.51	0.72	1.69	2.2	3.07
CaO	4.59	4.01	2.75	4.84	5.81	5.81	3.78	5.85	3.06	3.07	5.4	6.01	3.6	5.37	4.19	8.95
Na_2O	2.3	2.27	2.48	2.09	2	2.13	2.24	2.06	2.38	2.44	1.99	2.08	2.18	1.97	3.89	1.68
K_2O	3.37	3.21	3.44	3.11	2.22	2.14	3.26	2.35	3.37	3.69	2.64	2.21	3.11	2.24	3.39	2.83
P_2O_5	0.09	0.1	0.07	0.1	0.15	0.15	0.09	0.14	0.08	0.07	0.13	0.14	0.1	0.18	0.2	0.15
LOI	4.5	3.81	2.44	4.8	6.8	6.66	3.82	5.9	2.93	3.1	5.06	6.3	3.27	7.07	-	-
Total	100.02	99.98	100.35	99.98	99.57	99.63	99.98	99.5	100.07	99.6	99.83	99.66	99.56	99.53	-	100.8
CIA	48.9	47.9	47.57	50.07	55.27	53.51	48.83	50.93	47.71	47.28	50.13	51.29	48.04	54.58	-	-
PIA	48.35	46.86	46.38	50.1	56.94	54.57	48.25	51.27	46.56	45.81	50.18	51.72	47.06	56.09	-	-
CIW	38.69	37.56	37.24	40.25	49.18	47.43	38.65	43.32	37.26	36.06	41.2	44.24	37.67	48.16	-	-
Trace element (ppm)																
Li	18	14.7	15.1	17.7	31.4	29.9	15.4	21.3	11.7	12.6	17.9	22.6	12.5	28.2	20	-
Be	1.87	1.9	2.75	1.78	1.99	1.87	1.78	1.75	1.76	1.8	1.63	1.73	1.72	1.85	3	-
Sc	4.66	4.88	4.33	5.14	9.63	9.57	4.6	7.54	3.48	3.25	6.37	7.75	4.34	9.13	11	-
V	33	37.1	31.7	37.6	67.7	66.8	35.4	53.8	25.8	23.4	47.1	54	40.9	64.2	60	110
Cr	29	32.3	23.9	45.8	60.9	59.9	29	50.9	19.6	19.3	44.6	53	35.6	60.1	35	74
Co	40.6	46.7	81	47.3	20.4	23.6	45	31.5	73.5	54.3	39	28.8	48.9	27.9	10	-
Ni	15.5	15.4	14.2	22.8	27.8	26.5	14	19.5	11.3	10.7	17.2	21.1	12.4	25.7	20	40
Cu	9.02	8.37	7.35	9.86	18.3	17.2	8.61	12.5	6.26	6.22	10.7	13.2	7.6	17.9	25	40
Zn	28.8	26	24.2	29.8	51.3	49.3	25.6	36.3	19.2	19.4	31.6	38.3	22.7	53.4	71	65
Ga	11.7	11.9	15	11.7	13.4	13.1	11.5	11.3	11.1	11.4	10.9	11.4	10.8	12.9	17	16
Ge	0.94	1.11	1.32	1.08	1.2	1.22	0.97	1.1	0.82	0.82	1.08	1.1	0.89	1.24	1.6	-
Rb	121	118	155	114	91.5	88.2	114	87.2	115	124	95.9	83.9	104	87.9	112	110
Sr	310	332	462	298	216	223	313	247	329	337	264	232	302	218	350	385
Y	13.4	16.8	13.7	15.4	26.8	28.7	14.5	27.9	11.1	10.1	23.3	25.9	17.7	29.1	22	21
Zr	154	189	131	146	255	297	144	368	116	104	309	326	249	355	190	210
Nb	7.31	10.4	8.75	8.91	13.3	13.8	8.96	13.2	6.88	5.8	12.8	12.1	11.8	14.2	25	17
Cs	3.7	3.06	3.24	3.73	6.01	5.52	3.26	3.77	2.56	2.84	3.38	4.1	2.59	4.96	3.7	-

Table 3 (continued)

	WXM1	WXM2	WXS3	WXM4-1	WXM4-2	WXM4-3	WXM4-4	WXM4-5	WXM5	WXN7-2	WXN7-3	WXN7-4	WXN7-5	WXN7-6	UCC	WS
Ba	880	926	1298	831	463	466	879	555	934	988	697	507	852	501	550	480
Hf	3.67	4.52	3.21	3.51	6.31	7.34	3.43	8.82	2.76	2.58	7.44	7.92	5.69	8.62	5.8	-
Ta	0.66	0.95	0.93	0.81	1.01	1.05	0.81	1.09	0.78	0.59	1.11	0.97	1.09	1.09	1[a]	-
Pb	22.5	23.5	28.7	22.3	17.3	16.9	21.8	17.8	21.4	23.4	20	17	21.5	22.6	20	-
Th	5.98	8	6.7	6.74	9.66	10.1	6.7	10.5	5.34	4.98	10.2	9.3	9.29	11	10.7	17
U	1.28	1.58	1.42	1.46	2.39	2.67	1.49	2.57	1.09	1.05	2.19	2.43	1.71	2.73	2.8	-
Th/Sc	1.28	1.64	1.55	1.31	1	1.06	1.46	1.39	1.53	1.53	1.6	1.2	2.14	1.2	0.97	-
La/Sc	4.03	4.96	4.94	4.2	3.22	3.41	4.52	4.34	4.77	4.71	4.85	3.91	6.15	3.83	2.73	-
REE (ppm)																
La	18.8	24.2	21.4	21.6	31	32.6	20.8	32.7	16.6	15.3	30.9	30.3	26.7	35	30	28
Ce	32.8	44.2	38	38.5	62.4	66.7	38.3	64.8	29.6	26.2	60.5	59.5	52.6	69.4	64	59
Pr	4.06	5.43	4.59	4.76	7.09	7.57	4.64	7.49	3.65	3.23	7.08	6.86	6.05	7.97	7.1	-
Nd	15	20.3	17	17.8	27	28.3	17.2	28.2	13.6	11.8	26.4	25.9	22.2	29.7	26	-
Sm	2.8	3.72	3.08	3.28	5.21	5.52	3.22	5.4	2.49	2.14	4.96	5.03	4.03	5.71	4.5	-
Eu	0.7	0.85	0.84	0.79	1.04	1.07	0.76	1.03	0.65	0.62	1	0.98	0.85	1.09	0.88	-
Gd	2.51	3.29	2.75	2.97	4.76	5.03	2.84	4.85	2.18	2.02	4.43	4.59	3.51	5.18	3.8	-
Tb	0.36	0.46	0.38	0.42	0.71	0.75	0.4	0.72	0.31	0.28	0.64	0.68	0.49	0.77	0.64	-
Dy	2.18	2.83	2.27	2.57	4.37	4.67	2.42	4.44	1.82	1.66	3.84	4.21	2.94	4.64	3.5	-
Ho	0.43	0.55	0.45	0.5	0.86	0.94	0.47	0.88	0.36	0.33	0.76	0.83	0.57	0.94	0.8	-
Er	1.29	1.6	1.34	1.47	2.54	2.74	1.39	2.59	1.04	0.99	2.25	2.47	1.67	2.72	2.3	-
Tm	0.19	0.24	0.2	0.22	0.39	0.41	0.21	0.39	0.16	0.15	0.34	0.38	0.25	0.41	0.33	-
Yb	1.27	1.6	1.29	1.45	2.52	2.73	1.36	2.6	1.06	0.97	2.26	2.46	1.71	2.75	2.2	-
Lu	0.19	0.24	0.19	0.22	0.38	0.4	0.2	0.39	0.15	0.15	0.33	0.37	0.25	0.41	0.32	-
ΣREE	82.58	109.6	93.78	96.59	150.26	159.42	94.19	156.51	73.65	65.78	145.65	144.62	123.82	166.74	146.37	-
LRE E	74.15	98.79	84.91	86.76	133.73	141.76	84.9	139.64	66.56	59.26	130.79	128.62	112.43	148.92	132.48	-
HREE	8.43	10.81	8.87	9.83	16.53	17.66	9.29	16.87	7.08	6.53	14.86	15.99	11.39	17.82	13.89	-
LREE/HREE	8.79	9.14	9.57	8.82	8.09	8.03	9.14	8.28	9.4	9.08	8.8	8.04	9.87	8.36	9.54	-
La_N/Yb_N	1.08	1.11	1.22	1.09	0.9	0.88	1.12	0.92	1.15	1.16	1	0.9	1.14	0.93	1	-
Eu/Eu*	1.24	1.14	1.35	1.19	0.98	0.95	1.18	0.95	1.3	1.39	1	0.96	1.06	0.94	1	-
Ce/Ce*	0.86	0.88	0.87	0.87	0.96	0.97	0.89	0.94	0.87	0.85	0.93	0.94	0.94	0.95	1	-

LOI loss on ignition, *Fms* mud to silt, *Sfm* fine to medium sands, *Smc* medium to coarse sands, upper continental crust (UCC, Taylor and McLennan 1985); world sediment (WS, McLennan 1995).
[a] Updated in McLennan (2001)

Also provided are compositions of upper continental crust (UCC) and average world sediment (WS) for comparison

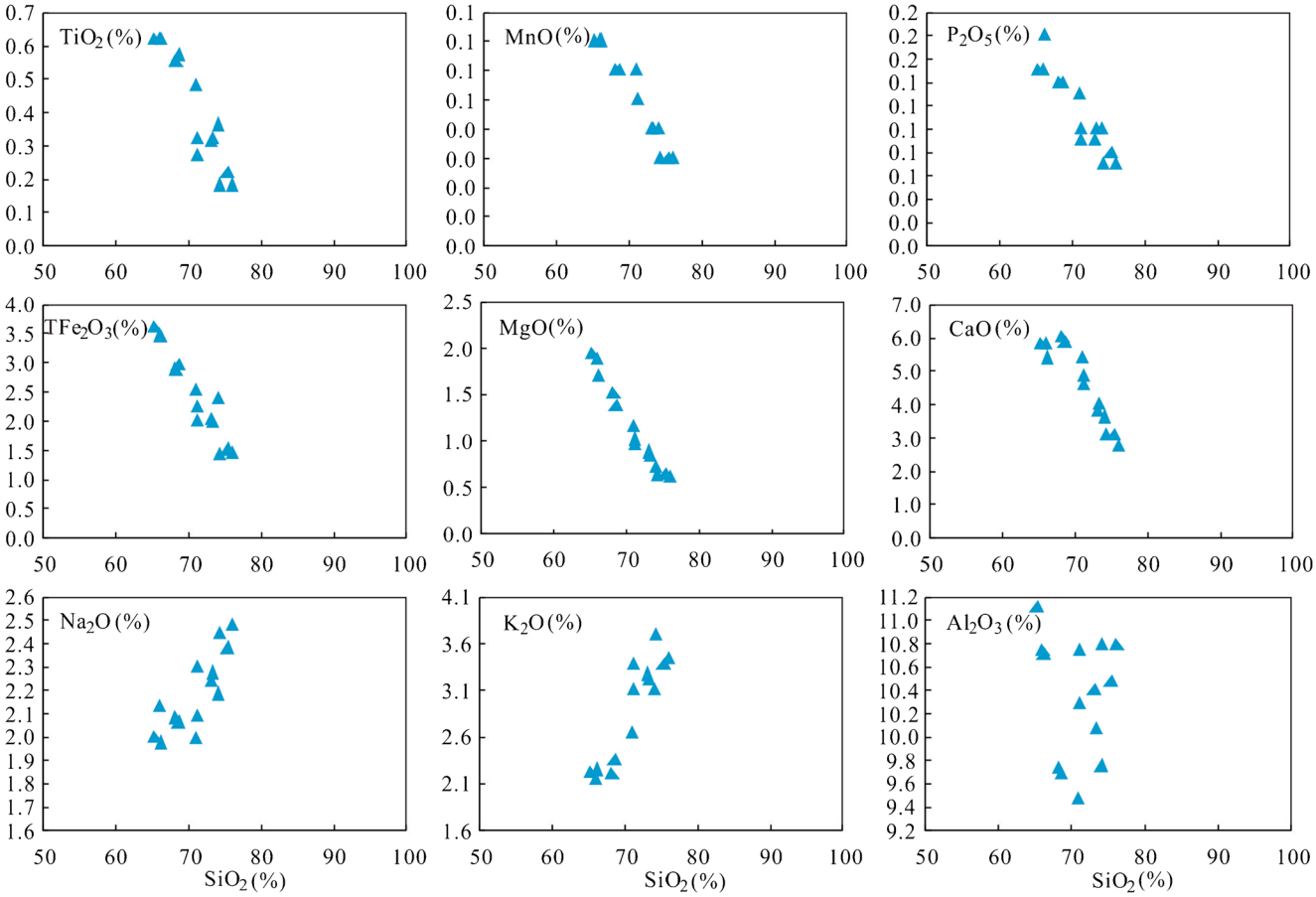

Fig. 3 Harker variation diagrams for major elements in the Weihe River sediments.

divided into two groups based on UCC-normalized REE distribution patterns (Fig. 6c,d). UCC-normalized REE values of silt samples (grain size between 4 and 62 μm) are mostly greater than 1, while UCC-normalized REE values of sand samples (grain size between 62 and 2000 μm) are less than 1 (Fig. 6c,d). Silt samples show similar distribution patterns as known average sediments S_{ave} and L_{ave} (Fig. 6c), suggesting the silty sediments were likely derived from the Loess Plateau to the north. Sand samples have REE patterns similar to the average composition of the granite from an upstream tributary, HG_{ave} (Fig. 6d). This indicates that sandy sediments are probably derived from the northern Qinling Mountain, where granite is widely distributed and which lies to the south of the Weihe River (Fig. 1). In addition, coarse sands and gravels deposited in the Feng and Ba Rivers, tributaries of the Weihe River (Fig. 1), are mainly granitic (Fig. 2e and f), supporting the above inferences on the sediment sources. Overall, provenance results indicate a bimodal source for sediments deposited along the Weihe River, a sedimentary source from the north that contributes fine-grained sediment, and a felsic igneous source form the south contributing coarser grained sediment.

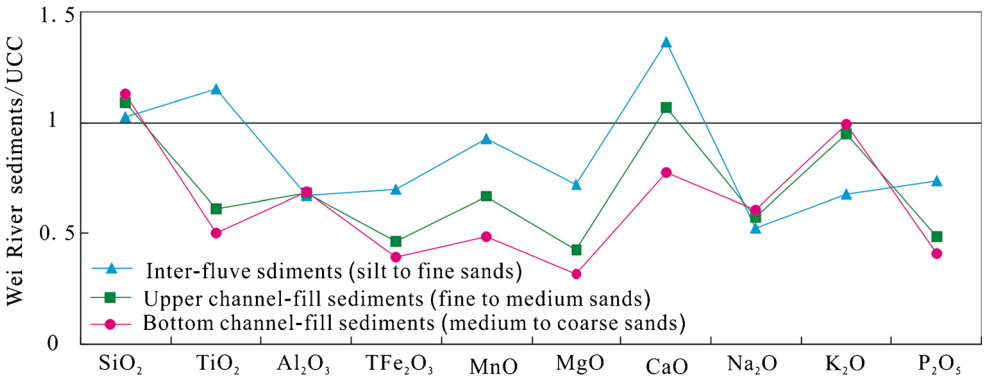

Fig. 4 Element ratios relative to Al_2O_3 for the channel-fill and inter-fluve sediments of the Weihe River calculated from average major element concentrations and normalized to UCC (Taylor and McLennan 1985)

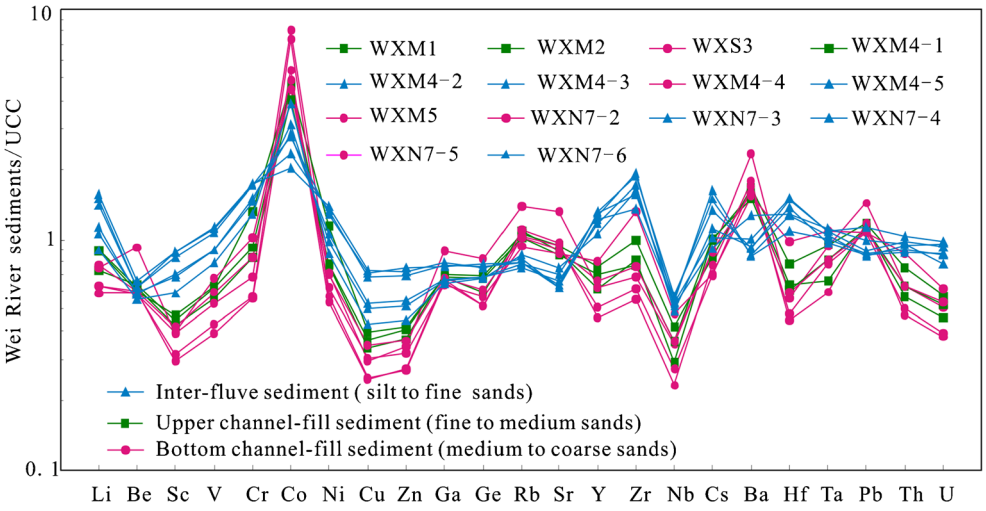

Fig. 5 Line diagram displaying average trace element concentrations of the Weihe River sediments normalized to UCC (Taylor and McLennan 1985). Elements are plotted in order of increasing atomic number (from left to right) (number of samples = 14)

Previous studies have demonstrated that the chemical composition of siliciclastic sedimentary rocks is a reflection of their source regions and can be used to characterize the source rocks from which the sediments were derived (e.g., Floyd and Leveridge 1987; Garver et al. 1996; Roser and Korsch 1988).

Table 4 Rare earth element abundances for the paleosol and loess of the Loess Plateau (Ding et al. 2001) and granite from upstream of the Hei River, Qinling Mountains (Lerch et al. 1995)

	S_{ave} (n = 8)	L_{ave} (n = 7)	HG_{ave} (n = 8)
La	37	35.7	24.74
Ce	74	71.4	47.05
Pr	8.59	8.21	4.75
Nd	32.8	31	16.64
Sm	6.66	6.39	2.98
Eu	1.38	1.31	0.7
Gd	6.31	5.9	2.31
Tb	0.92	0.87	0.36
Dy	5.48	5.17	2.3
Ho	1.1	1.06	0.33
Er	3.28	3.06	0.98
Tm	0.48	0.45	0.15
Yb	3.28	3	0.9
Lu	0.48	0.44	0.13
ΣREE	181.76	173.96	104.31
LREE	160.43	154.01	96.85
HREE	21.33	19.95	7.46
LREE/HREE	7.52	7.72	12.99
La_N/Yb_N	6.39	6.74	15.63
Eu/Eu*	0.73	0.72	0.88
Ce/Ce*	0.9	0.91	0.92

S_{ave} average paleosol in Loess Plateau (Ding et al. 2001), L_{ave} average loess in Loess Plateau (Ding et al. 2001), HG_{ave} average value of upper Hei River granite(Lerch et al. 1995)

The discriminant function analysis of Roser and Korsch (1988) has been carried out in order to investigate the provenance of the sediments collected along the Weihe River. Figure 7a shows the cross plot of these discrimination functions, with silty sediments plotting in the quartzose sediments of mature continental provenance zone, and most sandy sediments plotting in the felsic igneous provenance zone. A La/Th ratio and Hf abundance discrimination diagram (Fig. 7b), after Floyd and Leveridge (1987), indicates that acidic igneous rocks are the predominant sources of sandy sediments of the Weihe River sediments, and old sediment component are the predominant sources of silty sediments of the Weihe River sediments.

Paleoweathering

The mobilization, fractionation, and redistribution of major and trace elements are the primary results of weathering; and hence elements preserved in sedimentary rock can be used to reconstruct the paleoweathering intensity (Fritz and Mohr 1984; Nesbitt et al. 1997; Singh 2009). Several indices of weathering have been proposed based on the abundances of mobile and immobile oxides, including Na_2O, CaO, K_2O, and Al_2O_3. The chemical index of alteration (CIA; Nesbitt and Young 1982), plagioclase index of alteration (PIA; Fedo et al. 1995), and chemical index of weathering (Harnois 1988) are the most well-established methods for quantifying the degree of source weathering. The indices are defined as follows:

$$\mathrm{CIA} = \frac{\mathrm{Al_2O_3}}{\mathrm{Al_2O_3} + \mathrm{CaO}^* + \mathrm{Na_2O} + \mathrm{K_2O}} \times 100 \quad (1)$$

$$\mathrm{PIA} = \frac{\mathrm{Al_2O_3} - \mathrm{K_2O}}{\mathrm{Al_2O_3} + \mathrm{CaO}^* + \mathrm{Na_2O} + \mathrm{K_2O}} \times 100 \quad (2)$$

$$\mathrm{CIW} = \frac{\mathrm{Al_2O_3} - \mathrm{K_2O}}{\mathrm{Al_2O_3} + \mathrm{CaO}^* + \mathrm{Na_2O}} \times 100 \quad (3)$$

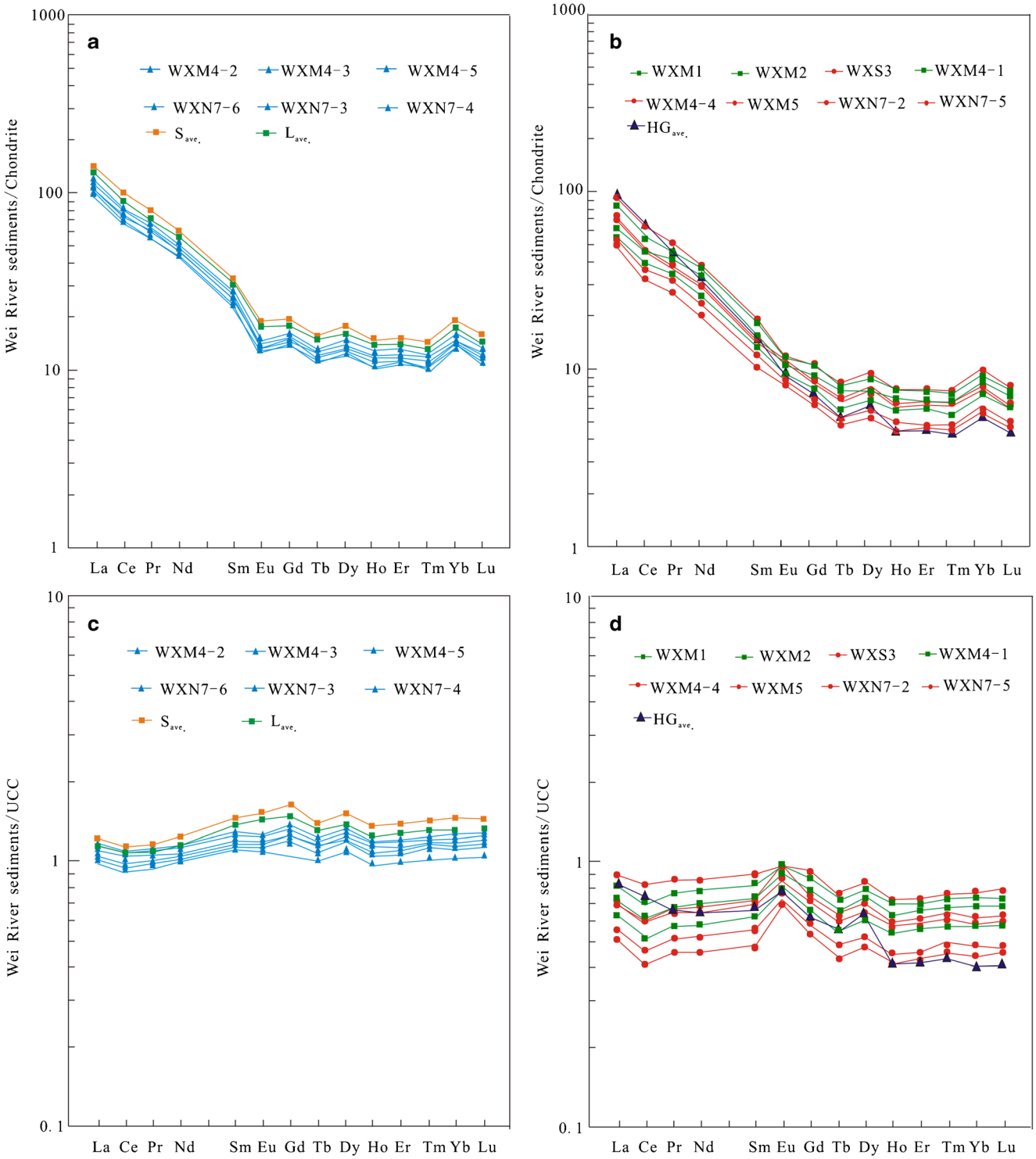

Fig. 6 Chondrite-normalized (Haskin et al. 1966) and upper continental crust (Taylor and McLennan 1985) normalized REE patterns of the Weihe River sediments from different depositional environments. Rare earth elements in inter-fluve sediments are most similar to UCC and show weak enrichments compared to UCC

where CaO* is the silicate-bearing minerals only.

There is no direct method for quantifying CaO*; however, McLennan et al. (1993) have proposed an indirect method for quantifying the CaO* fraction. The procedure for its quantification involves subtracting the molar abundance of P_2O_5 from the molar concentration of total CaO; if the remainder is

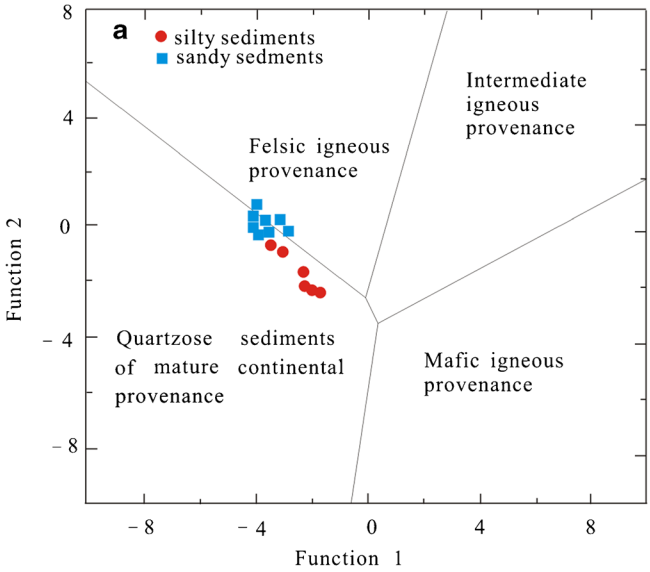

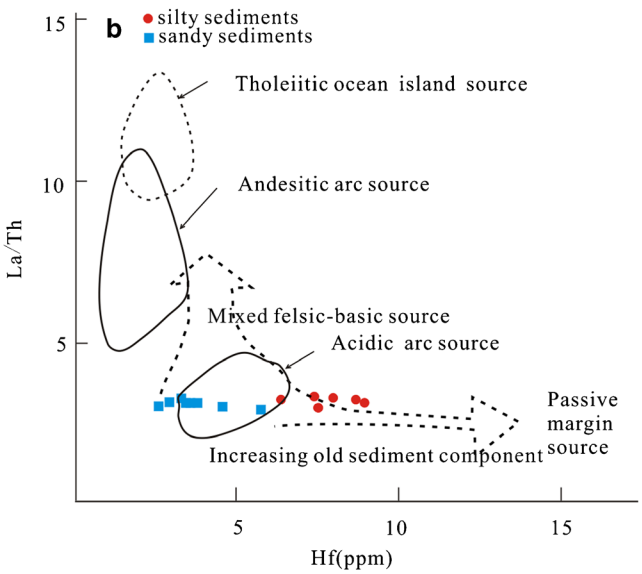

Fig. 7 **a** Provenance discrimination diagram for sediments of Weihe River sediments after Roser and Korsch (1988). Discriminant function1 = (−1.773 × TiO_2%) + (0.607 × Al_2O_3%) + (0.76 × $Fe_2O_3^T$%) + (−1.5 × MgO%) + (0.616 × CaO%) + (0.509 × Na_2O%) + (−1.22 × K_2O%) + (−9.09). Discriminant function 2 = (0.445 × TiO_2%) + (0.07 × Al_2O_3%) + (−0.25 × $Fe_2O_3^T$%) + (−1.142 × MgO%) + (0.432 × Na_2O%) + (1.426 × K_2O%) + (−6.861). **b** Discrimination plot of La/Th ratio and Hf abundance after Floyd and Leveridge (1987). Silt samples include WXM4-2, WXM4-3, WXM4-5, WXN7-3, WXN7-4, and WXN7-6, and sand samples include WXM-1, WXM-2, WXS3, WXM4-1, WXM4-4, WXM5, WXN7-2, and WXN7-5

greater than the molar concentration of Na_2O, then Na_2O is taken as the CaO* of silicate. If the remaining amount is less than the molar concentration of Na_2O, then CaO is considered to be representative of the silicate fraction (McLennan 1993; Moosavirad et al. 2011).

Following this procedure, the CIA, PIA, and CIW values for the Weihe River sediments have been determined, and the results are provided in Table 3. The CIA values vary from 47.28 to 55.27 (average = 50.14, n = 14). The CIA values of sandy sediments range from 47.28 to 50.07, whereas those in silty sediments range from 50.13 to 55.27. This indicates increasing weathering intensity from upstream to downstream, as would be expected. The low CIA values for the Weihe River sediments, ~ 50, indicate a relatively low degree of chemical weathering (Fedo et al. 1995). The mean CIA value for the Weihe River sediments is similar to that of UCC (CIA = 50.8; Sharma et al. 2013) and the Ganges River sediments (48–55) in the southwestern Himalayas (Singh 2010), suggesting a broadly analogous weathering regime.

The PIA and CIW range from 45.81 to 50.01 and 36.06 to 41.21, respectively (Table 3). Similar to the inference drawn from the CIA values, the PIA and CIW data for the Weihe River sediments also support a low degree of chemical weathering (Fedo et al. 1995). Residence time on flood plains has a strong influence on sediment composition, with longer residence times allowing for a greater intensity of chemical weathering (Johnsson 1993). Accordingly, the low values for the chemical weathering indices in the sandy sediments suggest less intense weathering, whereas low to moderate values in the silty sediments imply longer particle residence times and therefore a more intense, yet still relatively mild chemical weathering effect.

The low CIA, PIA, and CIW values in our samples may be attributed to the influx of minimally weathered detritus over short transport distances in a semi-arid environment. The short transport distance and semi-arid climate would have inhibited chemical weathering processes in the catchment. Silty sediments with a slightly higher, but still low CIA (50.13 to 55.27) from the Loess Plateau to the north may have allowed for water during flash flooding to percolate through source rocks, minimizing exposure to aqueous fluids, and thereby limiting the extent of chemical weathering.

Conclusion

Grain-size and outcrop analyses indicate that sediments from the Weihe River are predominantly silt (< 62 μm) and sand (62 μm to 2000 μm). Silty sediments are interpreted as an interchannel facies, while sandy sediments are interpreted as a channel-fill facies.

The Weihe River sediments are composed of silty and sandy sediments sourced from two distinct source regions adjacent to the Weihe River. Silty sediments are characterized by strong LREE enrichment relative to UCC, while sandy sediments are depleted relative to UCC. UCC-normalized REE distribution fingerprints, along with outcrop observations, discrimination functions and La/Th ratio and Hf

abundance discrimination diagram indicate that silty sediments of Weihe River are mainly derived from the Loess Plateau to the north, while sandy sediments are mainly derived from Qinling Mountains to the south.

The low CIA, PIA, and CIW values for fluvial sediments indicate the dominant source regions experienced relatively low degrees of chemical weathering. This work sheds important light on the geochemical composition, provenance, and chemical weathering of sediments that have contributed to the Weihe River catchment and established a baseline for future studies on the evolution of the Weihe River and for gauging the influence of anthropogenic activities, such as agriculture or other industrial activities, on the river system.

Acknowledgements Ling Guo is grateful to Wenbo Ren, Yu Zhu, and Jinchuan Duan (Department of Geology, Northwest University) for their assistance with sample collection.

Funding This study was sponsored jointly by the MOST Special Fund awarded by the State Key Laboratory of Continental Dynamics, Northwest University (201210128), the National Natural Science Foundation Project (41302076), Shandong Provincial Key Laboratory of Depositional Mineralization & Sedimentary Mineral, Shandong University of Science and Technology (DMSM2017033), and the Natural Science Basic Research Plan in Shaanxi Province of China (2014JQ5191).

References

Berner RA (1992) Weathering, plants, and the long-term carbon cycle. Geochim Cosmochim Acta 56(8):3225–3231

Bhatia MR (1983) Plate tectonics and geochemical composition of sandstones. J Geol 91(6):611–627

Bhuiyan MAH, Rahman MJJ, Dampare SB, Suzuki S (2011) Provenance, tectonics and source weathering of modern fluvial sediments of the Brahmaputra–Jamuna River, Bangladesh: Inference from geochemistry. J Geochem Explor 111(3):113–137

Condie KC, Noll JPD, Conway CM (1992) Geochemical and detrital mode evidence for two sources of Early Proterozoic sedimentary rocks from the Tonto Basin Supergroup, central Arizona. Sediment Geol 77(1-2):51–76

Cullers R (1988) Mineralogical and chemical changes of soil and stream sediment formed by intense weathering of the Danburg granite, Georgia, USA. Lithos 21(4):301–314

Ding ZL, Sun JM, Yang SL, Liu TS (2001) Geochemistry of the Pliocene red clay formation in the Chinese Loess Plateau and implications for its origin, source provenance and paleoclimate change. Geochim Cosmochim Acta 65(6):901–913

Fan SX (2014) Assessment of heavy metal pollution in stream sediments for the Baoji City section of the Weihe River in Northwest China. Water Sci Technol 70(7):1279–1284

Fedo CM, Eriksson KA, Krogstad EJ (1996) Geochemistry of shales from the Archean (~ 3.0 Ga) Buhwa Greenstone Belt, Zimbabwe: implications for provenance and source-area weathering. Geochim Cosmochim Acta 60(10):1751–1763

Fedo CM, Wayne Nesbitt H, Young GM (1995) Unraveling the effects of potassium metasomatism in sedimentary rocks and paleosols, with implications for paleoweathering conditions and provenance. Geology 23(10):921–924

Feng R, Kerrich R (1990) Geochemistry of fine-grained clastic sediments in the Archean Abitibi greenstone belt, Canada: implications for provenance and tectonic setting. Geochim Cosmochim Acta 54(4): 1061–1081

Floyd P, Leveridge B (1987) Tectonic environment of the Devonian Gramscatho basin, south Cornwall: framework mode and geochemical evidence from turbiditic sandstones. J Geol Soc 144(4):531–542

Fritz SJ, Mohr DW (1984) Chemical alteration in the micro weathering environment within a spheroidally-weathered anorthosite boulder. Geochim Cosmochim Acta 48(12):2527–2535

Gaillardet J, Dupré B, Louvat P, Allegre C (1999) Global silicate weathering and CO2 consumption rates deduced from the chemistry of large rivers. Chem Geol 159(1-4):3–30

Galloway WE, Hobday DK (1996) Fluvial Systems, Terrigenous Clastic Depositional Systems. Springer, pp 60–90

Garver J, Royce P, Smick T (1996) Chromium and nickel in shale of the Taconic foreland: a case study for the provenance of fine-grained sediments with an ultramafic source. J Sediment Res 100(1):100–106

Grantham JH, Velbel MA (1988) The influence of climate and topography on rock-fragment abundance in modern fluival sands of the southern Blue Ridge Mountains, North Carolina. J Sediment Res 58(2):219–227

Guo AL, Zhang GW, Sun YG, Cheng SY, Yao AP (2007) Geochemistry and spatial distribution of late-Paleozoic mafic volcanic rocks in the surrounding areas of the Gonghe Basin: Implications for Majixueshan triple-junction and east Paleotethyan archipelagic ocean. Sci China 50(2):292–304

Harnois L (1988) The CIW index: a new chemical index of weathering. Sediment Geol 55(3):319–322

Haskin LA, Wildeman TR, Frey FA, Collins KA, Keedy CR, Haskin MA (1966) Rare earths in sediments. J Geophys Res 71(24):6091–6105

Hessler AM, Lowe DR (2006) Weathering and sediment generation in the Archean: an integrated study of the evolution of siliciclastic sedimentary rocks of the 3.2 Ga Moodies Group, Barberton Greenstone Belt. South Africa. Precambrian Res 151:185–210

Johnsson MJ (1993) The system controlling the composition of clastic sediments. Geol Soc Am Spec Pap 284:1–20

Konhauser K, Fisher Q, Fyfe W, Longstaffe F, Powell M (1998) Authigenic mineralization and detrital clay binding by freshwater biofilms: the Brahmani River, India. Geomicrobiol J 15(3):209–222

Konhauser K, Fyfe W, Kronberg B (1994) Multi-element chemistry of some Amazonian waters and soils. Chem Geol 111(1):155–175

Kronberg B, Fyfe W, Leonardos O, Santos A (1979) The chemistry of some Brazilian soils: element mobility during intense weathering. Chem Geol 24(3):211–229

Liu Y, Liu XM, Hu ZC, Diwu CR, Yuan HL, Gao S (2007) Evaluation of accuracy and long-term stability of determination of 37 trace elements in geological samples by ICP-MS. Acta Petrol Sin 23(5): 1203–1210

Lei K, Lu XW, Wang LJ, Zhai YX, Huang J, Qu YZ (2008) Distribution and evaluation on potential ecological risk of heavy metals in Wei River surface sediment of Xi'an. Geo Sci Technol Inf 27(3):83–87

Lerch M, Xue F, Kröner A, Zhang G, Tod W (1995) A middle Silurian-Early Devonian magmatic arc in the Qinling Mountains of central China. J Geol 437-449

Li PY, Qian H, Wu JH, Chen J, Zhang YQ, Zhang HB (2014) Occurrence and hydrogeochemistry of fluoride in alluvial aquifer of Weihe River, China. Environ Earth Sci 71(7):3133–3145

Li Y, Fang J, Yuan XY, Chen YY, Yang HB (2018) Distribution Characteristics and Ecological Risk Assessment of Tetracyclines Pollution in the Weihe River, China. Int J Enviro Res Public Health 15(1803):1–11

Liu S, Li Q, Zhang L (2009) Geology, geochemistry of metamorphic volcanic rock suite in precambrian Yejishan Group, Lüliang mountains and its tectonic implications. Acta Petrol Sin 25(3):547–560

Manikyamba C, Kerrich R, González-Álvarez I, Mathur R, Khanna TC (2008) Geochemistry of Paleoproterozoic black shales from the Intracontinental Cuddapah basin, India: implications for provenance, tectonic setting, and weathering intensity. Precambr Res 162(3):424–440

Mao L, Mo D, Yang J, Guo Y, Lv H (2014) Rare earth elements geochemistry in surface floodplain sediments from the Xiangjiang River, middle reach of Changjiang River, China. Quat Int 336:80–88

McCann T (1998) Sandstone composition and provenance of the Rotliegend of the NE German Basin. Sediment Geol 116(3-4): 177–198

McLennan SM (1993) Weathering and global denudation. J Geol 101: 295–303

McLennan SM (1995) Sediments and soils: chemistry and abundances. A Handbook of Physical Constants: Rock Physics and Phase Relations: American Geophysical Union, Reference Shelf Series 3: 8–19

McLennan SM (2001) Relationships between the trace element composition of sedimentary rocks and upper continental crust. Geochemistry Geophys Geosystems 2(4):1021–1024

McLennan SM, Taylor S, Kröner A (1983) Geochemical evolution of Archean shales from South Africa. I. The Swaziland and Pongola Supergroups. Precambrian Res 22(1-2):93–124

McLennan S, Hemming S, McDaniel D, Hanson G (1993) Geochemical approaches to sedimentation, provenance, and tectonics. Geol Soc Am Spec Pap 284:21–40

Meybeck M (1987) Global chemical weathering of surficial rocks estimated from river dissolved loads. Am J Sci 287(5):401–428

Moosavirad S, Janardhana M, Sethumadhav M, Moghadam M, Shankara M (2011) Geochemistry of lower Jurassic shales of the Shemshak Formation, Kerman Province, Central Iran: provenance, source weathering and tectonic setting. Chemie Erde-Geochem 71(3): 279–288

Nesbitt H, Young G, McLennan S, Keays R (1996) Effects of chemical weathering and sorting on the petrogenesis of siliciclastic sediments, with implications for provenance studies. J Geol 104(5):525–542

Nesbitt HW, Fedo CM, Young GM (1997) Quartz and feldspar stability, steady and non-steady-state weathering, and petrogenesis of siliciclastic sands and muds. J Geol 105(2):173–192

Nesbitt HW, Young G (1982) Early Proterozoic climates and plate motions inferred from major element chemistry of lutites. Nature 299(5885):715

Oliva P, Viers J, Dupré B (2003) Chemical weathering in granitic environments. Chem Geol 202(3-4):225–256

Price JR, Velbel MA (2003) Chemical weathering indices applied to weathering profiles developed on heterogeneous felsic metamorphic parent rocks. Chem Geol 202(3-4):397–416

Rahman MJJ, Suzuki S (2007) Geochemistry of sandstones from the Miocene Surma Group, Bengal Basin, Bangladesh: Implications for Provenance, tectonic setting and wealthering. Geochem J 41(6):415–428

Rollinson HR (2014) Using geochemical data: evaluation, presentation, interpretation. Routledge

Roser B, Korsch R (1988) Provenance signatures of sandstone-mudstone suites determined using discriminant function analysis of major-element data. Chem Geol 67(1):119–139

Sharma A, Sensarma S, Kumar K, Khanna P, Saini N (2013) Mineralogy and geochemistry of the Mahi River sediments in tectonically active western India: implications for Deccan large igneous province source, weathering and mobility of elements in a semi-arid climate. Geochim Cosmochim Acta 104:63–83

Singh P (2009) Major, trace and REE geochemistry of the Ganga River sediments: Influence of provenance and sedimentary processes. Chem Geol 266(3):242–255

Singh P (2010) Geochemistry and provenance of stream sediments of the Ganga River and its major tributaries in the Himalayan region, India. Chem Geol 269(3):220–236

Stallard RF (1995) Tectonic, environmental, and human aspects of weathering and erosion: a global review using a steady-state perspective. Annu Rev Earth Planet Sci 23(1):11–39

Sugitani K, Yamashita F, Nagaoka T, Yamamoto K, Minami M, Mimura K, Suzuki K (2006) Geochemistry and sedimentary petrology of Archean clastic sedimentary rocks at Mt. Goldsworthy, Pilbara Craton, Western Australia: evidence for the early evolution of continental crust and hydrothermal alteration. Precambrian Res 147(1-2):124–147

Taylor SR, McLennan SM (1985) The continental crust: its composition and evolution. Blackwell Scientific Pub, Palo Alto

Tripathi JK, Ghazanfari P, Rajamani V, Tandon S (2007) Geochemistry of sediments of the Ganges alluvial plains: evidence of large-scale sediment recycling. Quat Int 159(1):119–130

Velbel MA (1993) Temperature dependence of silicate weathering in nature: how strong a negative feedback on long-term accumulation of atmospheric CO2 and global greenhouse warming? Geology 21(12):1059–1062

Wang T, Sun G, Liu S (2011) Relationship between spatiotemporal variation of water pollution and runoff volume of mainstream section of the Weihe River in Shaanxi Province. Arid Zone Res 28(4):599–615

Whitmore GP, Crook KA, Johnson DP (2004) Grain size control of mineralogy and geochemistry in modern river sediment, New Guinea collision, Papua New Guinea. Sediment Geol 171(1):129–157

You QY, Jiang H, Liu Y, Liu Z, Guan ZL (2019) Probability analysis and control of river runoff-sediment characteristics based on pair-copula functions: the case of the Weihe River and Jinghe River. Water 11(3):510–529

Zhang GW, Zhang BR, Yuan XC, Xiao QH (2001) Qinling orogenic belt and continental dynamics. Sci. Press, Beijing, pp 1–806

Zhang H, Lu H, Jiang SY, Vandenberghe J, Wang S, Cosgrove R (2012a) Provenance of loess deposits in the Eastern Qinling Mountains (central China) and their implications for the paleoenvironment. Quat Sci Rev 43:94–102

Zhang YZ, Huang CC, Pang JL, Zha XC, Zhou YL, Yin SY, Wang J (2012b) Comparative study of the modern flood slackwater deposits in the upper reaches of Hanjiang and Weihe River Valleys, China. Quat Int 282:184–191

Zhang Z, Wang X, Zhang Y, Nan Z, Shen B (2012c) The over polluted water quality assessment of Weihe River based on kernel density estimation. Procedia Environ Sci 13:1271–1282